Why pancreatic islets burst but single β cells do not

The heterogeneity hypothesis

Paul Smolen, John Rinzel, and Arthur Sherman
Mathematical Research Branch, National Institute of Diabetes and Digestive and Kidney Diseases, National Institutes of Health, Bethesda, Maryland 20892 USA

ABSTRACT Previous mathematical modeling of β cell electrical activity has involved single cells or, recently, clusters of identical cells. Here we model clusters of heterogeneous cells that differ in size, channel density, and other parameters. We use gap-junctional electrical coupling, with conductances determined by an experimental histogram. We find that, for reasonable parameter distributions, only a small proportion of isolated β cells will burst when uncoupled, at any given value of a glucose-sensing parameter. However, a coupled, heterogeneous cluster of such cells, if sufficiently large (~125 cells), will burst synchronously. Small clusters of such cells will burst only with low probability. In large clusters, the dynamics of intracellular calcium compare well with experiments. Also, these clusters possess a dose–response curve of increasing average electrical activity with respect to a glucose-sensing parameter that is sharp when the cluster is coupled, but shallow when the cluster is decoupled into individual cells. This is in agreement with comparative experiments on cells in suspension and islets.

INTRODUCTION

Pancreatic β cells naturally exist in an electrically-coupled network, the islet of Langerhans. A long-standing question is to what extent the electrical and secretory responses of β cells to glucose are properties of individual cells or of the islet. The bulk of experimental evidence indicates that β cell–bursting electrical activity depends on gap-junctional coupling (1, 2). There is also direct evidence that coupling enhances insulin secretion (3). Some have emphasized the contribution of population heterogeneity (4). Here we present new theoretical results that may shed light on these questions.

Most experimental reports describe bursting only in intact islets or sufficiently large clusters (1). The one report of normal-appearing bursts (although with a very long period) from isolated β-cells (5) has yet to be replicated. The recording was obtained at a higher temperature (30°C vs room temperature) and with a different patch clamp technique (Nystatin-perforated patch vs whole-cell patch) than most other experiments on isolated cells. Typically, isolated β cells exhibit depolarization and irregular spiking in elevated glucose (1, 2).

To account for the difference between isolated cell and intact islet behaviors, Atwater and colleagues (6) proposed the channel-sharing hypothesis, which held that current fluctuations caused by individual channel openings would prevent bursting. Cells coupled by gap junctions in islets, however, would feel reduced fluctuations because of current spread to neighbors, allowing expression of the underlying burst dynamics. We (7, 8) and others (9) found support for this idea in simulations of clusters with stochastic channels.

Here we consider an alternative hypothesis, motivated in part by the observation that bursting in single-cell models (7, 10) is quite sensitive to parameter values. Outside a narrow parameter regime, model cells remain silent, spike continuously, or exhibit bursts with unphysiological characteristics. If pancreatic β cells are likewise sensitive and are variable, bursting might be rare among isolated cells. On the other hand, because of coupling, cells within an islet, despite their individual differences, behave as a unified collective. Bursting, a slow alternation between spiking and quiescence, could occur as the oscillating compromise among cells which would be either steadily active or silent if isolated.

In contrast to systems based on pacemaker cells, this proposed mechanism does not require a subpopulation of bursting cells. Bursting results from cooperation of cells with different properties, each of which alone produces a much simpler form of activity.

We have tested this hypothesis by simulating a heterogeneous population of model cells, using experimental data on variability of β cell size (11), gap-junctional conductances (12), and ionic channel densities (1, 5, 13). We find that, with only ~10% variance in parameter values, most of our individual cells are either tonically active, or silent, with few (~5%) bursting at a given glucose level. Coupling a mixture of such cells readily leads to synchronized bursting (see Fig. 2) in adequately sized clusters, say of 125 cells.

Coupling heterogeneous cells also addresses our concerns about parameter sensitivity: although the population mean values of parameters remain constrained for bursting, the ensemble tolerates considerable variability in the parameter values of individual cells.

We cannot exclude the possibility that the observed differences in behavior between isolated cells and islets are experimental artifacts. We assume, however, that the differences are genuine and search for physiological explanations. Independent of this, our model provides useful insights into the functioning of heterogeneous cell populations.

Address correspondence to Dr. Paul Smolen, Mathematical Research Branch, National Institute of Diabetes and Digestive and Kidney Diseases, Building 31, Room 4B-54, National Institutes of Health, Bethesda, MD 20892, USA.

0006-3495/93/06/1668/13 $2.00

As an application of the model, we examine the proposition that heterogeneity underlies the glucose dose–response properties of pancreatic islets (14–16). According to this hypothesis, there is a distribution of thresholds for glucose response (14). The thresholds may apply to the onset of electrical activity of cells or the exocytotic release of insulin granules from cells. As the glucose increases, the less responsive cells or pools are recruited. Simulations of populations of noninteracting cells reveal only a weak response to glucose. When cells are coupled, however, so that they respond as a unit, sharp dose–response curves are obtained, in agreement with the experiment. Thus, at least with respect to electrical activity and Ca_i levels, the key to glucose sensing does not seem to be heterogeneity per se, but coupling, which overcomes heterogeneity to permit synchronized activity, and the dynamics of bursting.

MODELING AND METHODS

Single-cell model

Previous studies with coupling were based on a Chay–Keizer single-cell model (17) as modified by Sherman et al. (7). However, recent whole-cell electrophysiological data (18, 19) concerning the details of calcium currents appear incompatible with activation parameter values of that model. Also, whereas in the Chay–Keizer type models bursting results from slow accumulation and removal of intracellular Ca^{2+}, intracellular Ca^{2+} has now been visualized with dyes (20, 21) and it appears that calcium varies rapidly relative to burst duration. A newer single-cell model (10) incorporates the recent data on Ca^{2+} currents and does not rely on slow variation in intracellular Ca^{2+}. Rather, as previously proposed (22), bursting is driven by a slowly varying ATP-modulated potassium (K-ATP) conductance. With one modification, we use this model for individual cells in our clusters.

We do not want to focus on whether the adopted model faithfully represents the β cell in all respects. Indeed, the behavior of this model is sensitive to the existence of small currents at negative membrane potentials (10), and there is question as to whether such currents have been completely quantified by the protocols of Hopkins et al. (18), Satin and Cook (19), or others. Also one group (5) has failed to detect a slowly varying K-ATP conductance during bursting. Rather, in the absence of consensus as to the correct mechanism for bursting, we look for model-independent features by comparing results with those using an earlier, modified Chay–Keizer model (7, 8).

Model parameters are as in Fig. 6 of reference 10 except as indicated below. The capacitance, ionic currents, and conductances are defined as densities, per unit area of cell surface.

The current balance equation is

$$C_m \frac{dV}{dt} = -I_{ion}, \tag{1}$$

where I_{ion} is the sum of several Ca^{2+} and K^+ currents:

$$I_{ion} = I_{Ca,f}(V, p_{ca,o}) + I_{Ca,s}(V, J) + I_{Ca,l}(V) + I_{K-dr}(V, n, I) + I_{K-ATP}(V). \tag{2}$$

The delayed rectifier current, $I_{K-dr} = \bar{g}_K n I (V - V_K)$, activates on a ~20 ms time scale, with open probability, n, satisfying

$$\frac{dn}{dt} = \lambda\left[\frac{n_\infty(V) - n}{\tau_n(V)}\right], \tag{3}$$

and it inactivates slowly (time scale ~5 s),

$$\frac{dI}{dt} = \frac{I_\infty(V) - I}{\tau_I(V)}. \tag{4}$$

The model incorporates two V-dependent Ca^{2+} currents, $I_{Ca,f}$ and $I_{Ca,s}$, (18) and there is a small, V-independent Ca^{2+} leak current (23). Each Ca^{2+} current is a product of the conductance and a Goldman–Hodgkin–Katz driving force that neglects dependence on Ca_i, the concentration of intracellular Ca^{2+}:

$$I_{Ca,f} = g_{fast}\phi(V) \quad I_{Ca,s} = g_{slow}\phi(V) \quad I_{Ca,l} = \bar{g}_{leak}\phi(V), \tag{5}$$

$$\phi(V) = Ca_o \frac{V}{\left[1 - \exp\left(\frac{V}{13.35}\right)\right]}. \tag{6}$$

$I_{Ca,s}$ activates instantaneously and inactivates slowly (~10 s):

$$g_{slow} = \bar{g}_{Ca}(1 - X_f)m_\infty(V)J, \tag{7}$$

$$\frac{dJ}{dt} = \frac{J_\infty(V) - J}{\tau_J(V)}. \tag{8}$$

The kinetics of $I_{Ca,f}$ depend on both voltage-gated activation and fast (~100 ms) inactivation by Ca^{2+}, incorporated in the open probability, $p_{ca,o}$:

$$g_{fast} = \bar{g}_{Ca} X_f p_{ca,o}. \tag{9}$$

See reference 10 for details of $p_{ca,o}$ kinetics. The parameter X_f partitions the Ca^{2+} conductance into components that inactivate rapidly or slowly.

Although I and J represent slow processes, in this model bursting is primarily driven by slow oscillations in [ATP] and [ADP]. During the active phase, increased Ca_i inhibits ATP production (22):

$$\frac{d[\text{ATP}]}{dt} = k_a\left\{\exp\left[R\left(1 - \frac{Ca_i}{R_1}\right)\right][\text{ADP}] - [\text{ATP}]\right\}. \tag{10}$$

[ATP] + [ADP] = A is assumed constant, thus [ADP] rises during the active phase, leading to an increase in I_{K-ATP},

$$I_{K-ATP} = \bar{g}_{K-ATP} \frac{1 + \frac{[\text{ADP}]}{K_1}}{1 + \frac{[\text{ADP}]}{K_1} + \frac{[\text{ATP}]}{K_2}}(V - V_K), \tag{11}$$

which terminates the burst and repolarizes the cell. The rate of ATP synthesis increases with R, which is considered as the glucose-sensing parameter, increasing with glucose. Ca_i is determined by a balance of influx and removal:

$$\frac{dCa_i}{dt} = f\left[-\frac{3}{2Fr}(I_{Ca,f} + I_{Ca,s} + I_{Ca,l}) - k_{Ca}Ca_i\right]. \tag{12}$$

Here F is Faraday's constant and r is the cell radius.

When simulations were run with a heterogeneous cluster, Ca^{2+} levels in some cells rose to ≥ 1 μM. To prevent this, we postulated an additional mechanism of Ca^{2+} uptake from the cytosol, which only becomes significant at high Ca^{2+}. We add the following Hill function to the right-hand side of Eq. 12:

TABLE 1 **Parameters that are distributed**

$C_m = 10.0$ fF μm^{-2}
$X_f = 0.27$
$\bar{g}_{K-ATP} = 9.744$ pS μm^{-2}
$r = 7.0$ μm
$k_{Ca} = 0.12$ ms^{-1}
$A = 1.0$ mM
$\bar{g}_{Ca} = 6.685$ pS mM^{-1} μm^{-2}
$\bar{g}_{leak} = 28.58$ fS mM^{-1} μm^{-2}
$\bar{g}_K = 8.120$ pS μm^{-2}
$R = 0.49$
$k_a = 0.035$ s^{-1}

* Parameters not listed here are identical to reference 10, Fig. 6. In contrast to reference 10, conductances and capacitance are per unit area here.

$$-f\bar{Q}\frac{Ca_i^N}{K_{upt} + Ca_i^N}. \qquad (13)$$

Standard values of some parameters are listed in Tables 1 and 2. The values of other parameters not shown above, and the form of functions such as n_∞, τ_n, et cetera may be found in reference 10.

For comparison, some studies were done using a modified Chay-Keizer model (7, 8) for individual cells instead.

Numerical methods

The method for integration of the equations for a cluster of cells has been previously described (8). We use Heun's method (a predictor-corrector form of the trapezoidal rule) with a time step $\Delta t = 0.1$ ms; some calculations were repeated with $\Delta t = 0.01$ ms to check that sufficient accuracy had been attained. Computations were performed on a Cray YMP computer, which allowed vectorizing the computation over cells to keep computing time within reason. As our model cluster, we used a $5 \times 5 \times 5$ cube of cells. This is smaller than an islet, but represents a compromise with available computing power; 150 s of problem time takes ~15 min of central processing unit time.

Modeling cell heterogeneity

For simulations, cell heterogeneity is implemented by normally distributing the parameters in Table 1. Gaussian random variables are generated with the Box-Mueller algorithm.

Experimental data on parameter variability are available for only a few parameters, specifically cell size and channel conductances. Fluorescence-activated cell sorting has been used to quantify the distribution of size of dispersed β cells from rat islets (4, 11). We distribute the cell radii in a Gaussian manner. Then the resulting distribution of cell surface area is skewed and has a tail at large volumes, as does the experimental distribution. We assume a standard deviation of 8% of the mean for the distribution of radii. Then, approximately two thirds of the cells have surface area within 17% of the mean, similar to experiment (11).

Total conductances and C_m increase with surface area, whereas parameters such as k_{Ca}, the rate constant for Ca^{2+} removal, do not. In addition, C_m might vary because of differences in membrane composition, and is distributed. Similarly, conductances are distributed because of differences in channel density. Rorsman and Trube (1) estimated the standard deviation of the whole-cell Ca^{2+} conductance in mouse β cells, and that of the K^+ conductance due to the delayed-rectifier channel. They divided by the cell capacitance, providing a rough measure of channel density distribution. Standard deviations on the order of 10% are suggested by this data. The distribution of ATP-dependent K^+ channel density is not well characterized, but the input conductance of different β cells in the absence and presence of glucose has been examined (5, 13) and the variation is significant, probably ~10–20% of the mean. Because this input conductance is mainly due to the ATP-dependent K^+ channel in the absence of glucose, these data provide an estimate of the K – ATP conductance distribution if the cell capacitance is relatively constant. The leak conductance, $\bar{g}_{leak}$, was assigned a standard deviation of 15%.

The remaining parameters in Table 1, such as k_{Ca}, or the glucose-sensing parameter R, depend on numbers of transporters, electron-transport proteins, et cetera, and, although not yet experimentally characterized, are also expected to vary. We assume standard deviations of 10%. Our qualitative results do not depend on the precise values of these standard deviations.

Parameters in Table 2 are kept uniform over the cell population. The parameter λ, for example, is a property of a particular molecular species, i.e., a particular ion channel, and would only vary if this molecule were subject to differing influences capable of altering its conformation; we neglect this possibility. Other molecular parameters are found in steady state inactivation and activation expressions and, because they are always constant at the values given in Fig. 6 of reference 10, they are not listed here. We have simplified by keeping Ca_o, the extracellular Ca^{2+} concentration, the same for all cells, although Ca_o (and K_o) are likely to vary in a real cluster.

Heterogeneous coupling

To model a cluster of β cells, we index the single-cell equations by cell number, j, and add to the current-balance equation the gap-junctional current, which is proportional to the voltage difference between cells:

$$C_{mj}\frac{dV_j}{dt} = -I_{ion,j} + \sum_{k \in N} g_{jk}(V_k - V_j). \qquad (14)$$

The summation is over the neighbors k of cell j. In a cubic lattice, interior cells have six neighbors, exterior cells fewer. Heretofore, we have considered coupling conductances between all cells identical (8). However, this conductance between β cells in isolated pairs varies greatly, according to Perez-Armendariz et al. (12), who measured electrical coupling between pairs of β cells dispersed from mouse islets. They constructed a histogram showing that ~35% of pairs were uncoupled, and that the conductance of coupled pairs varied from 25 to 600 pS, with a mean and standard deviation of 215 and 110 pS, respectively.

To simulate this histogram ("Perez histogram"), we divide the interval (0, 1) into subintervals whose lengths equal the fractions of cells having coupling conductances within corresponding 25 pS-wide subintervals of the histogram. Then, to assign each coupling conductance, we call a random number generator to pick from a uniform distribution on (0, 1) and assign the conductance on the basis of the subinterval

TABLE 2 **Parameters that are uniform over cells**

$V_K = -75$ mV
$Ca_o = 2.5$ mM
$\bar{Q} = 0.12$ μM ms^{-1}
$\lambda = 0.84$
$K_{upt} = 0.6$ μM
$N = 3$

* Parameters not listed here are identical to reference 10, Fig. 6. In contrast to reference 10, conductances and capacitance are per unit area here.

in which the number falls. It is necessary to ensure subsequently that $g_{jk} = g_{kj}$.

We neglect the effect of gap-junctional current on Ca_i because, unless gap junctions select for Ca^{2+}, K^+ and Na^+ would carry most of this current because of their much higher concentrations. Thus, the effect on Ca_i would be small. We also neglect possible diffusion of ATP and ADP through gap junctions, and any correlation between coupling conductance and cell size. Finally, we neglect possible dependence of gap-junctional coupling on glucose level, although evidence for this exists (24).

Results

Bursting in a heterogeneous cluster

In Fig. 1 *A* we show bursting for an isolated cell in the model of Smolen and Keizer (10). The time course of Ca_i (Fig. 1 *B*) is also burstlike; and its sharp upstroke and magnitude are consistent with recent experiments visualizing Ca_i with Ca^{2+}-sensitive dyes (20, 21). The slow variable that drives the bursts is (ADP) (Fig. 1 *C*). The voltage bursts have a smooth envelope of spiking which tends to "pinch in" just after the beginning of the burst. This feature, which is not seen experimentally, appears in the model to be related to inactivation of Ca^{2+} currents by Ca^{2+}. The pinching cannot be eliminated by tuning parameters while remaining faithful to the voltage-clamp currents, which include Ca^{2+}-mediated inactivation.

For the cluster simulations, we added a Ca^{2+}-damping term (Eq. 13), as explained in Modeling and Methods. Also, because coupling changes burst characteristics such as plateau fraction and spike amplitude, some parameters (C_m, R, λ) were adjusted to values (Tables 1 and 2) that result in reasonable bursts for coupled clusters. Interestingly, with this standard set of parameters, a single cell does not burst but remains at a hyperpolarized steady state (not shown).

If the parameters are distributed, as described in Modeling and Methods, but the cells are not coupled, very few cells, 4, burst; 69 cells are silent, and 52 spike continuously. Fig. 2, *A–C* shows the voltage time course of three cells in the cluster, one silent, one bursting, and one continuously spiking. The large spike amplitudes in Fig. 2, *B* and *C* are a consequence of the low value of λ, 0.84.

We coupled the cells using conductances determined by the Perez histogram (12). Fig. 2, *D–F* shows the voltage time courses in the coupled cluster for the same cells as in Fig. 2, *A–C*. Almost all the cells in this cluster burst with bursts of physiological appearance. The low value of λ, which generates very large spikes in isolated cells, gives acceptable spikes here. This effect of coupling to diminish spike height has been noted previously (8, 25). The pinching seen in the single-cell model (Fig. 1 *A*) disappears completely when the cells are coupled. The spike height varies rapidly within a burst. Such variability, present in most experimental records from islets (26; 27; and reference 28, Fig. 4.1) is not produced by any single-cell, deterministic model. This irregularity, also seen in reference 29, is purely deterministic; note that there is no jitter in the silent phase, in contrast to reference 8, where stochastic channel events play a role.

We modeled 20 variants of this cluster, identical except for the seed for the random number generator used to assign parameters and coupling conductances. All these clusters exhibited coordinated bursting, with the great majority of cells bursting. Within a few variant clusters phase differences among cells exceeded 1/10 of a burst period, and some bursts had odd appearances, unlike most published records. Occasionally, small spikes during the silent phase were seen, reflecting coupling to more active neighbors. There are a few published (reference 28, Fig. 4.12 B; reference 30, Fig. 5.2) records resembling our odd simulated bursts. Within most cluster variants, however, the bursts looked like those in Fig. 2, *D–F*.

The bursts are synchronized among cells, but spiking is not. Corresponding bursts of different cells have different numbers of spikes, with different shapes. Fig. 2 *G* shows spikes at the beginning of a burst for two cells that are not nearest neighbors. Although not apparent in Fig. 2 *G*, spiking is somewhat correlated among cells as indicated by the spikes in the time course of V averaged over the cluster (Fig. 2 *H*). In contrast, averaged V for the uncoupled cluster of Fig. 2, *A–C* (not shown) is essentially flat.

Another view of the effects of coupling is the scatter plot (Fig. 3) of the oscillation amplitudes of V and [ADP] for the cells. In the uncoupled cluster the silent cells (Fig. 2 *A*) have $\Delta V = 0$ and Δ[ADP] = 0. The continuously spiking cells have Δ[ADP] near zero but nonzero ΔV (Fig. 2 *C*). Only the four bursting cells are marked by a significant Δ[ADP], generated by silent-to-active transitions. In the coupled case, all but one of the cells bursts.

In the cluster, [ADP] oscillations (not shown) are similar to those in single cells (Fig. 1 *C*). [ADP] levels vary from cell to cell. Fig. 1 *D* shows the time course of Ca_i averaged over the cluster. This average measure corresponds to experiments in which islets are loaded with a Ca^{2+}-sensitive dye (20, 21), and more closely resembles the experimental results than does Fig. 1 *B* in that the spikes on the plateau are smaller. This is because the voltage spikes are smaller and because the cells spike asynchronously.

Robustness of bursting

One of our initial motivations was to make bursting more robust with respect to parameter variation. We have seen that coupling may allow bursting in a cluster even if few cells can burst when isolated. Roughly, the

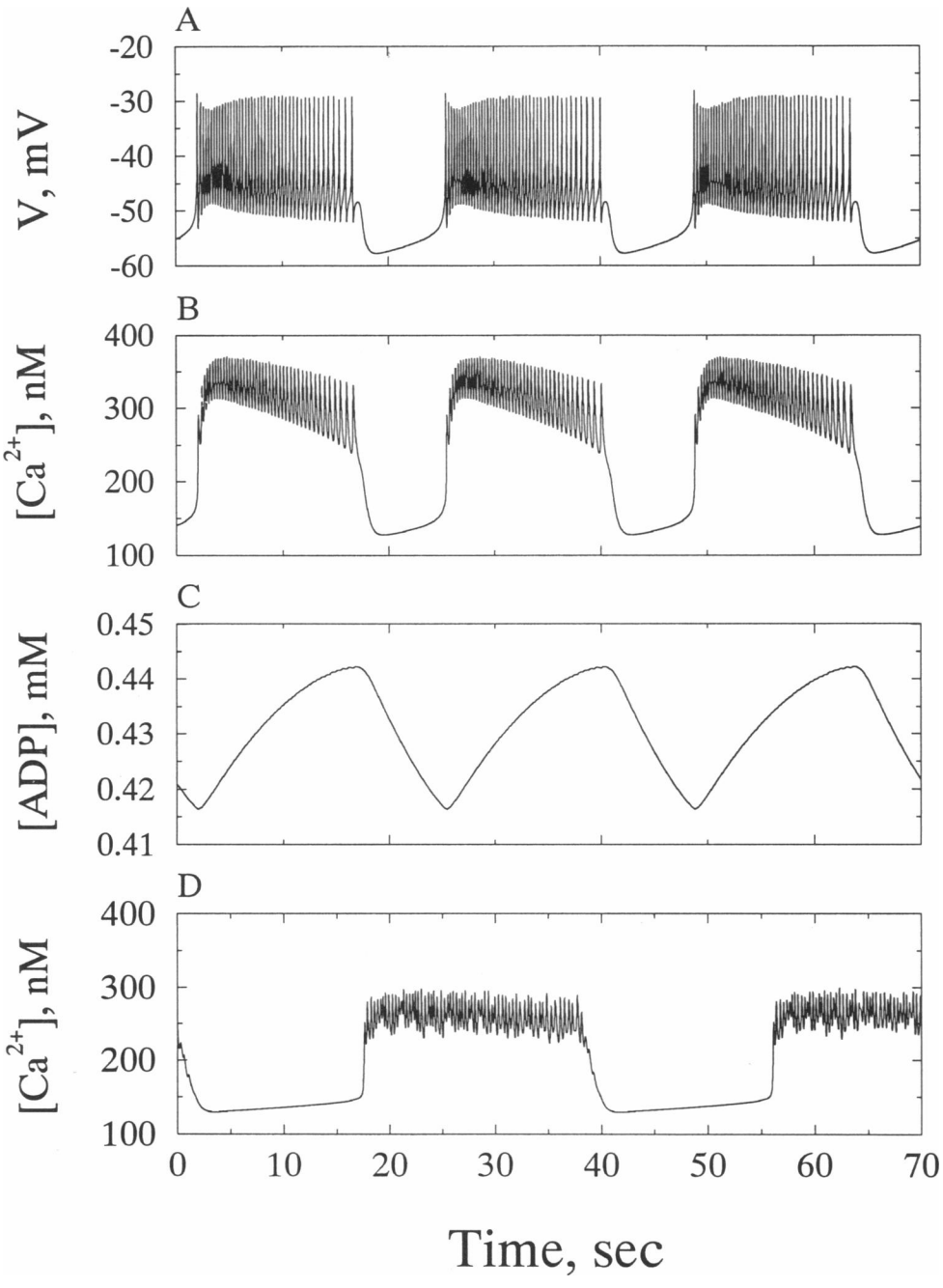

FIGURE 1 Bursting of the model of Smolen and Keizer (10). Parameters are as in reference 10, Fig. 6. Membrane potential (*A*), intracellular [Ca^{2+}] (*B*), and intracellular [ADP] (*C*) are shown for a solitary β cell. *D* shows the time course of [Ca^{2+}] averaged over all cells in the coupled $5 \times 5 \times 5$ cluster of Fig. 2, *D–F*.

cluster bursts if the population mean values of parameters are near the bursting regime for a single cell. Individual cells in a bursting cluster may be far from the mean and far from values that allow bursting without coupling. In this sense, bursting is more robust, because population means vary less than values for the individual cells.

The behavior of the cluster cannot be completely predicted from that of an isolated cell with the mean parameters (the mean cell). For example, Fig. 5 shows heterogeneous clusters as in Fig. 2, but with a range of values for the mean of R, $\bar{R}$. The range of values of $\bar{R}$ that supports bursting for a cluster is left shifted relative to the mean cell. In particular, the mean cell corresponding to the cluster in Fig. 2 ($\bar{R} = 0.49$) would be silent if isolated.

In Fig. 5, coupling expands the parameter regime for bursting, but with different choices of other parameters, such as $\bar{g}_{Ca}$, this would not necessarily hold. We

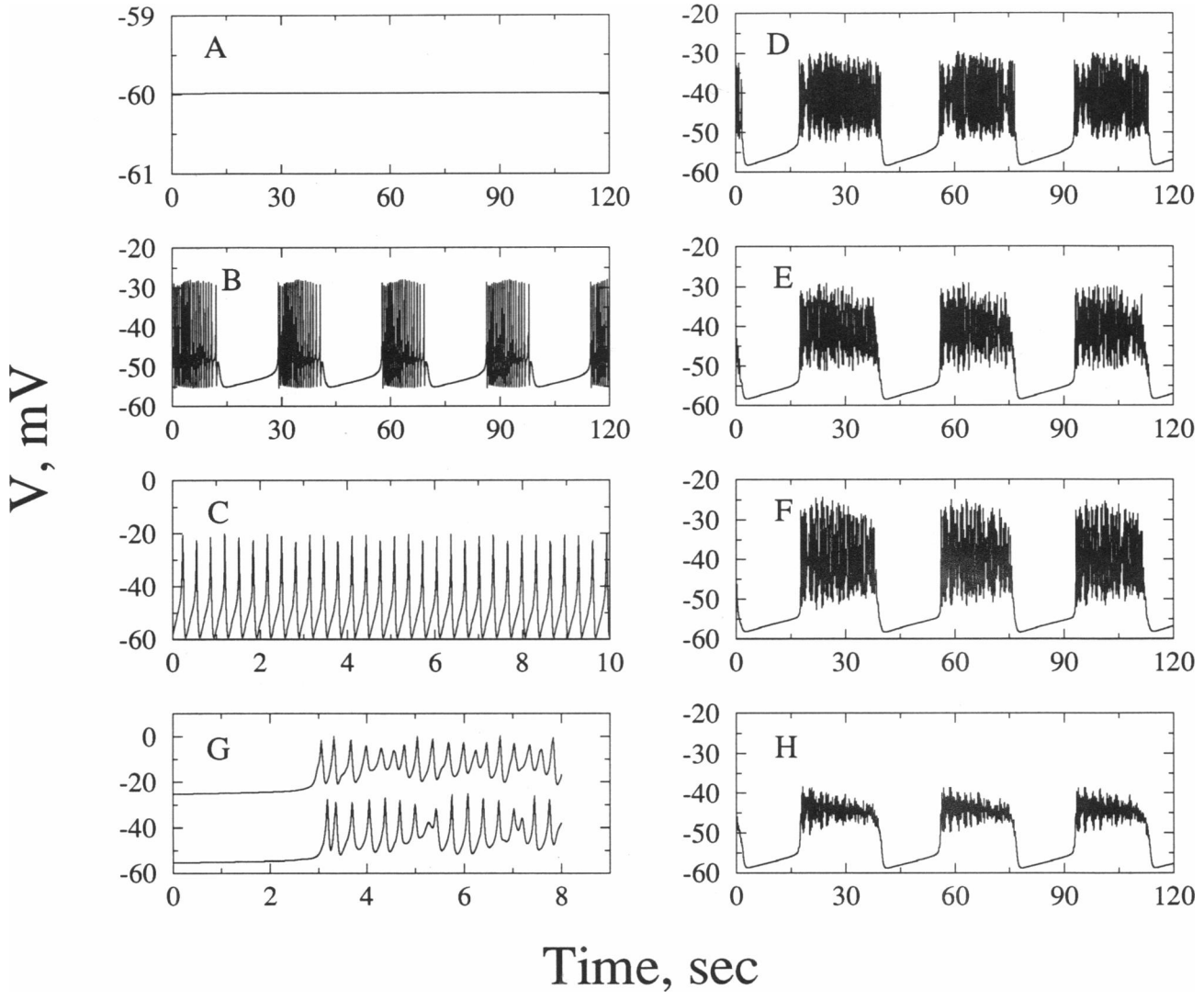

FIGURE 2 Synchronized bursting due to electrical coupling of heterogeneous β cells in a $5 \times 5 \times 5$ cluster. Membrane potential time courses for selected cells, uncoupled (*left*) and coupled (*right*). Uncoupled, only four cells burst; the rest are either silent (69 cells) or continuously active (52 cells). Those that burst have large spikes. Three cells, not nearest neighbors, are shown. Uncoupled, one is silent (*A*), one bursting (*B*), and one continuously spiking (*C*). Nearest-neighbor coupling induces synchronized bursting of the entire cluster. The same three cells coupled are shown in *D*, *E*, and *F*. *G* magnifies the leading spikes in a burst from the cells in *E* (offset by +30 mV) and *F*; spikes are not synchronized. *H* shows the time course of the average voltage of all cells in the coupled cluster.

tested this with clusters in which just two parameters were distributed, R and $\bar{g}_{Ca}$. As in Fig. 5, the cluster could burst in some cases where the mean cell could not but failed to burst in some cases where the mean cell could. With this broader view, however, it was apparent that although coupling changed the shape of the burst region, it did not cause an overall increase in area. Thus, although robustness is enhanced in that each cell need not be in the burst regime, the mean must still lie in a relatively small region of parameter space.

In particular, coupled clusters are sensitive to variations in the mean channel densities, especially $\bar{g}_{Ca}$. This sensitivity is significantly greater when the single-channel current-voltage relation is given by the Goldman–Hodgkin–Katz formula, which permits single-channel rectification, rather than the strictly linear Ohm's law relationship.

Small clusters

In cultured clusters of 5–10 mouse β cells, ragged bursts with short (5 s) and variable periods are observed experimentally (L. Satin, personal communication). There is one exceptional report of long well-defined bursts (5). Simulations with homogeneous, uniformly coupled clusters of stochastic cells (7, 8) indeed produce noisier

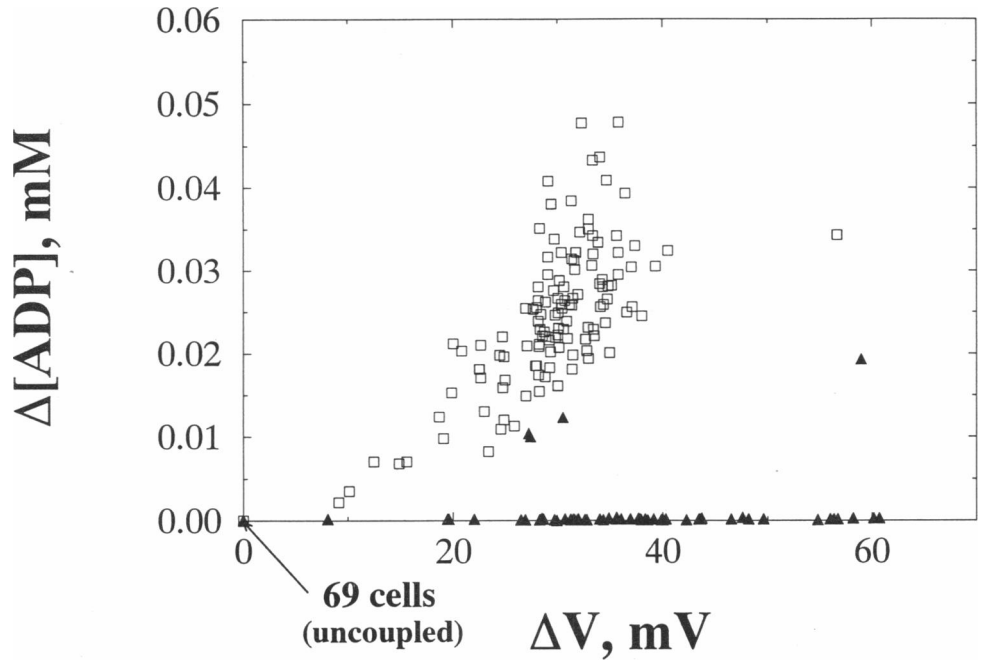

FIGURE 3 Characterization of behavior (bursting or otherwise) for all cells in the coupled vs uncoupled 125-cell cluster. Points show Δ[ADP], the difference between maximum and minimum [ADP] within a 100-s interval, vs ΔV, the difference between maximum and minimum voltages, for each cell in the cluster. Uncoupled cells (*filled triangles*); coupled cells (*open squares*). In the uncoupled cluster, 69 cells are silent, having both Δ[ADP] and $\Delta V = 0$. Cells with Δ[ADP] = 0 and ΔV not zero are continuously spiking. Only four uncoupled cells burst. Upon coupling, most cells burst and move to a larger Δ[ADP], occupying a region of roughly $20 < \Delta V < 40$, $0.01 < \Delta[\text{ADP}] < 0.04$.

bursts when cluster size is small, say <50. As cluster size decreases, the bursts become noisier and degenerate into irregular spiking, so that no cell in a 5–10 cell cluster can be said to burst.

With small heterogeneous coupled clusters, lacking channel noise, we find a different pattern than in the stochastic simulations. We simulated 30 independent trials (different seeds for the random number generator) with a $2 \times 2 \times 2$ cube. Cell parameters and coupling conductances were distributed as for Fig. 2. Of the clusters that could be unambiguously classified, five burst, 11 were continuously active, and 11 were silent. Small clusters are more liable to sample error and thus less likely to burst than large clusters. Three clusters could not be classified because both bursting and continuous spiking were present. One expects poorer synchronization in small clusters because of the smaller number of connections of boundary cells. Because parameter space is less well sampled within a small cluster the burst patterns also vary widely from cluster to cluster. For example, two clusters had bursts with almost no spikes.

Thus, whereas the stochastic model predicts a gradual degradation of burst quality as population size decreases, the bursts in the heterogeneous, noise-free model do not degrade, but rather fewer bursting clusters are found. Because heterogeneity does not explain the noisy bursting observed experimentally in small clusters, channel noise, or experimental conditions such as temperature, may be important factors.

Dependence of synchrony on coupling strength

Previous simulations with homogeneous, uniformly coupled, stochastic clusters (8) showed that burst period is not monotonic with respect to coupling strength, but achieves a maximum well above its value at very weak or strong coupling. When coupling is very strong, spikes, as well as bursts, synchronize and the behavior of the cluster is identical to that of a single cell with the same parameter values. We report here similar computations with heterogeneous clusters. Parameters were assigned as in Fig. 2, but the mean of R was raised to 0.56 to keep the cluster from becoming silent at very strong coupling. Coupling was made uniform for all cells for comparison with earlier work. To assess the synchrony of bursting, we plotted the time course of the fraction of cells active, f_A, with "active" defined as $V > -53$ mV.

For no coupling, f_A is constant with small random fluctuations (Fig. 4 *A*), reflecting the lack of synchrony among the continuously active cells; almost no cells burst. With very weak coupling of 25 pS, there is some synchrony (Fig. 4 *B*). The crest-to-trough amplitude of the f_A oscillations shows that about one-third of the cells are bursting together. At 50 pS (Fig. 4 *C*), most cells are

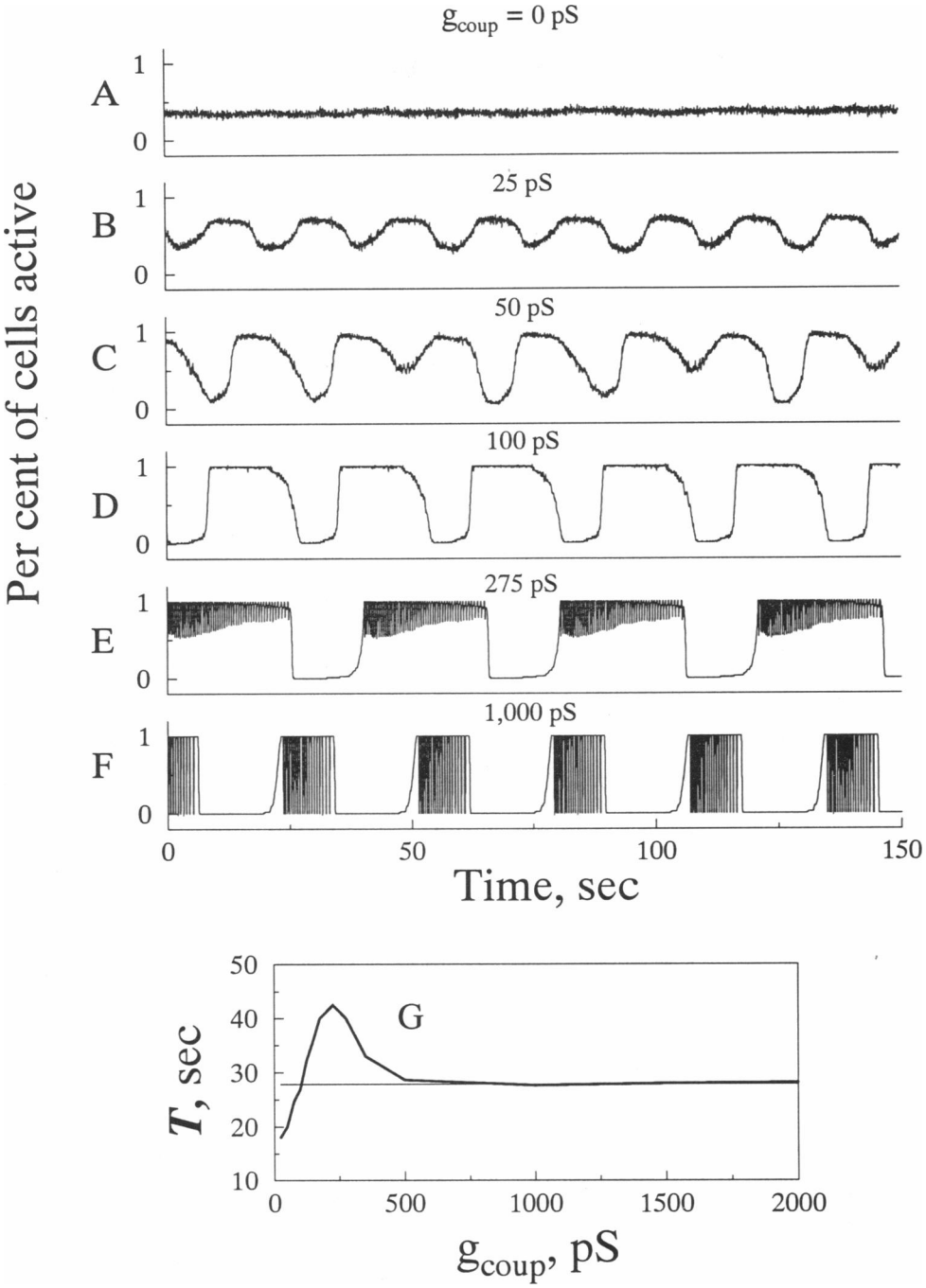

FIGURE 4 Degree of synchrony increases in a 125-cell cluster of heterogeneous β cells with increasing uniform coupling strength. Cell parameters are as in Fig. 2, except mean R is increased to 0.56. A–F show percent of cells active ($V > -53$ mV) vs time for gap junctional conductance g_c = 0, 25, 50, 100, 275, and 1000 pS, respectively. Burst synchronization is virtually complete at 100 pS, but spike synchronization requires stronger coupling. G shows the burst period T versus coupling strength. Period is maximized for coupling in the physiological range; the maximum occurs at about g_c = 225 pS and exceeds by 50% the period for infinitely strong coupling. The horizontal line indicates the period of the mean cell of the cluster.

bursting with weak synchrony. At times, nearly all cells are active or silent, but the rounded shape of the oscillation indicates wide variation in plateau fraction among cells. An unusual pattern, with one group of cells bursting every other period, is seen. At g_c = 100 pS (Fig. 4 D) all cells are bursting synchronously, with f_A oscillating between 0 and 1, corresponding to all cells silent and active, respectively. A similar approximate coupling threshold was found for synchronization of bursting with identical, noisy cells (8). Plateau fraction now varies little among cells. The rounded transitions between active and silent phases reflect phase-lag across the clus-

ter. As g_c is increased above 100 pS, the burst period increases significantly. At 275 pS (Fig. 4 *E*) spikes have appeared in the time course of f_A. This reflects synchronization of the voltage spikes among all the cells; the base of the spikes in some cells is now below −53 mV. Finally, at very high coupling (1,000 pS) the spikes are well synchronized in all cells and are large (similar to Fig. 2 *B*), all dipping below −53 mV, so that f_A spikes from 0 to 1 (Fig. 4 *F*). Unlike in homogeneous clusters (8), other variables such as Ca_i and [ADP] do not equalize because Ca_i and [ADP] handling parameters are distributed.

The dependence of burst period on coupling conductance is summarized in Fig. 4 *G*. As in homogeneous clusters, there is a maximum at intermediate coupling. The maximum is ~50% greater than either that at very strong coupling or that of the cluster's mean cell, which bursts at the increased value of R here. At very large g_c burst period asymptotes to a value near, but not identical to, that of the mean cell.

The above phenomena depend on the strength, not the form, of the coupling; similar results were obtained by scaling the nonuniform g_c's of the Perez histogram.

For uniform coupling of $g_c \approx 200$ pS we found a slow modulation of the spike envelope. See also reference 29, Fig. 2. This phenomenon, not reported in experiments, appears to be a transitional stage between the rapid spike modulation seen with heterogeneous coupling (Fig. 2, *D–F*) and the unmodulated, perfectly synchronized spikes seen at very strong coupling.

Glucose dose–response properties

We can use the heterogeneous cluster model to study the implications of cell variability for glucose dose–response behavior. Pipeleers and co-workers (4, 11, 16) summarized differences in the electrical responses of β cells (31) and in their metabolic redox states (32). Although we do not model a cell's redox state, we can simulate the effects of glucose on intracellular [ADP] and Ca_i. Increased glucose is modeled as increased ATP synthesis rate, R (10, 22). We measure glucose response by Ca_i, averaged over cells and over time, versus $\bar{R}$, and by the population mean plateau fraction (fraction of time spent in the active phase of bursting) versus $\bar{R}$, the mean of R. Plateau fraction (26) correlates with the rate of insulin secretion, and, in the model, Ca_i correlates with plateau fraction.

The main result (Fig. 5) is that the dose–response curve for the coupled cluster (*filled circles*) is much steeper than that for the uncoupled cluster (*filled squares*). The uncoupled configuration corresponds to an experiment (3) with isolated cells in suspension. Plateau fraction (not shown) behaves similarly.

The dose–response curves for both the coupled and uncoupled clusters are bracketed by a range of Ca_i levels within which the middle two thirds of the cells fall. The range for the uncoupled cluster (*dashed lines*) is much broader than for the coupled cluster (*shaded region*). There is substantial variation of Ca_i levels among cells even in the coupled case. The [ADP] distribution (not shown) is little affected by changing $\bar{R}$ within the bursting range.

We also show the dose–response curve for the mean cell of the cluster (*open circles*), illustrating that the cluster's behavior is not simply determined by that of the mean cell. The cluster has a left-shifted curve and also substantially higher Ca_i levels.

DISCUSSION

We have explored a new hypothesis for why few (or no) isolated β cells burst although bursting is robustly observed in mouse islets. We postulated that because of cell heterogeneity, most cells have parameters outside the narrow range that supports bursting, but that coupling would allow populations of cells to cooperate and achieve bursting. The bursting regime is narrow in these models because bursting depends on a delicate balance of small currents.

We have confirmed by simulations that distributing parameters with a standard deviation as small as 10–20%, as reported experimentally, is enough to prevent bursting in all but a few randomly chosen cells (Figs. 2, *A–C* and 3). Most cells were either silent (hyperpolarized) or continuously spiking, although steady depolarization was also seen. Coupling of physiologically plausible extent and strength, however, readily led to synchronized bursting (Figs. 2, *D–F* and 3) in large clusters (125 cells). This held even with no gap junctions between 35% of nearest-neighbor pairs. The bursts looked realistic in that their spike heights varied rapidly, somewhat like experimental records. In the intermediate case of small clusters (eight cells), bursting was seen only rarely. We have replicated our qualitative results with a second, rather different model for β cell electrophysiology, a modified Chay–Keizer model (7), suggesting that the results are not model dependent.

Bursts are generated in heterogeneous clusters by balancing silent and active cells. Consider the simplified case of two cells. Choose parameters such that, when uncoupled, one cell is silent and one continuously spiking. (For example, adjust the glucose-sensing parameter R.) Now couple the cells strongly so that they have the same V, or nearly so. Then, unless the spiker or the silent cell is strongly dominant, the pair will not remain either spiking or silent, but will instead cycle periodically between the two states, i.e., burst. When they are both silent, the more excitable cell will slowly depolarize the pair until they cross threshold and begin to spike. When they are both spiking, the less excitable cell will cause an eventual repolarization.

For coupled clusters, the collective behavior can be silent, bursting, or continuously spiking, depending on

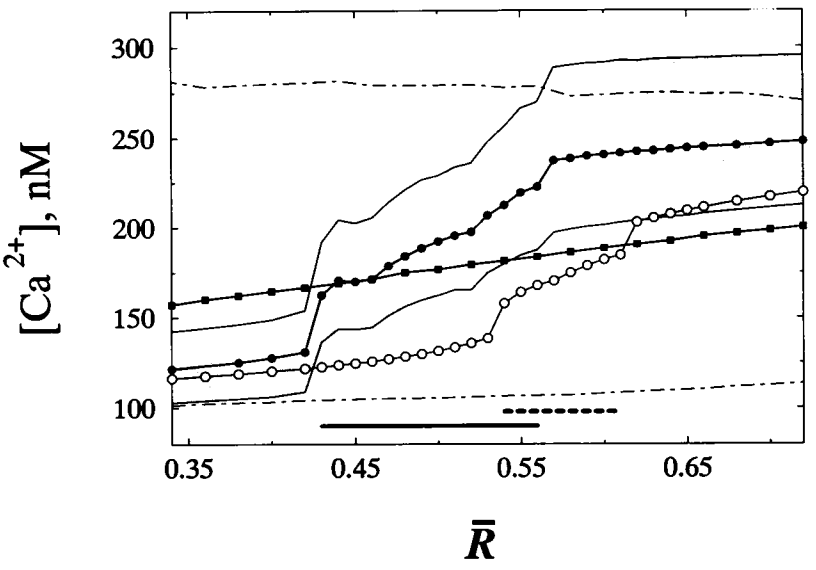

FIGURE 5 Glucose dose–response curves for the heterogeneous cluster and its mean cell. Increasing glucose is modeled by increasing R, or its mean value, $\bar{R}$ for the cluster. The response is in terms of intracellular $[Ca^{2+}]$ averaged over 140 s and over cells, for coupled (*filled circles*) and uncoupled (*filled squares*) clusters. The gray region includes time-averaged $[Ca^{2+}]$ of two thirds of the cells in the coupled cluster. The analogous region for the uncoupled case is bounded by the two dashed curves. The dose–response curve for the coupled cluster is steeper, and $[Ca^{2+}]$ much less variable. Fig. 2 corresponds to the case $\bar{R} = 0.49$. The cluster curve is broadened and left-shifted relative to the mean cell (*open circles*). Bursting regime for the cluster is indicated by the solid horizontal bar above the abscissa and for the mean cell by the dashed bar.

the proportions of intrinsically (i.e., when isolated) silent and continuously active cells. For example, in Fig. 5, the mean value of R for the cluster, $\bar{R}$, is varied. At low $\bar{R}$, most of the cells are intrinsically silent, and so is the coupled cluster. As $\bar{R}$ increases, some silent cells become active. When the ratio of intrinsically active to silent cells reaches ~1:2, the cluster begins to burst. The plateau fraction of the bursts increases with $\bar{R}$, until the ratio of active to silent reaches ~1:1, when the cluster goes into continuous spiking (plateau fraction is 1).

In the absence of coupling, as the silent cells convert to spikers with increasing $\bar{R}$, most pass through a narrow regime of bursting. However, at any given level of $\bar{R}$ few cells burst. These bursters are not necessary for the coupled cluster to burst: they can be removed with little effect. Nor are they sufficient: if too many of the cells are intrinsically silent, a few bursters scattered randomly can not drive the cluster to burst, but are suppressed by the silent cells. The three-dimensional character of our clusters (and real islets) means that the bursters are electrotonically close to a large conductance load. In our simulations, a minority of bursters could initiate a wave of bursting in a silent majority only if they were grouped together spatially and partially electrically isolated, by making coupling strength implausibly small or by making the cluster one dimensional.

This differs from pacemaker systems, such as the heart, in which a subpopulation of cells capable of oscillating on their own drives the rest. Nor can the continuously active cells be said to drive the slow oscillation; the contribution of both active and silent groups is needed.

In single-cell models, bursting depends on bistability in the underlying spike-generating mechanism between a depolarized active state and a hyperpolarized silent state, as well as a slow process (here, variation of ADP; see Fig. 1) to switch between them (7, 10). Cells in a cluster must still meet this requirement. For example, coupling two standard Hodgkin–Huxley-type neurons, with applied bias currents such that one cell is at rest and one oscillatory, would not suffice to give bursting, because there is no slow process to switch spiking on and off.

Rhythmogenesis by parameter mixing of active and silent cells is also applicable to simpler models, such as coupled excitable cells, one excited and one at rest, of the Fitzhhugh–Nagumo type (33). A similar idea was also proposed (34) to explain how adding a small number of periodically secreting *Dictyostelium* amoebae to a population of mutant chaotic secreters suppresses the chaos.

Although the behavior of clusters differs from that of their mean cells (Fig. 5), roughly speaking, clusters burst if their mean parameters are near the bursting regime. Because the mean varies less from cluster to cluster than the values for individual cells, coupling enhances the robustness of bursting. It is still the case, however, that the mean values of some parameters, particularly conductances, have to fall within narrow ranges for bursting to be obtained. Fig. 5 shows that the range of mean values

of R that supports bursting is expanded by coupling, but for some other combinations of parameter values the range is diminished.

The "stochastic channel-sharing hypothesis" (7, 8) offered another reason why single cells could not burst: channel noise, especially from large-conductance Ca^{2+}-activated K^+ (K-Ca) channels, may disrupt the bursts. It has lost favor because of evidence that blocking K-Ca channels with charybdotoxin has little effect on bursting in islets (35) and because some higher-temperature, perforated patch recordings from single cells show noise-free activity (5). The stochastic and heterogeneity hypotheses are not mutually exclusive, and may both be relevant.

Both hypotheses predict that sufficiently large, sufficiently well-coupled clusters will burst, but they also differ in some ways. For small coupling strength one finds noisy, tonic spiking in the stochastic case, and a division of the population into spikers, silent cells, and (a few) bursters in the heterogeneous case. As cluster size, N, decreases the bursts gradually degrade in the stochastic case as the perturbing effects of channel fluctuations are enhanced (7, 8). In the heterogeneous case small cluster size results in poorer sampling of the parameter space. Typically, a small cluster either has well-defined bursts or does not burst at all, but the probability of bursting declines with N. This is a prediction that could be tested by systematic electrical recordings from clusters of different sizes.

In both cases spike amplitude is reduced by the coupling interactions because the spikes are not synchronized even though the bursts are. Compare Fig. 2, *B* and *E*, and also see reference 8, Fig. 5. One lesson is that some details of the individual cell dynamics, such as the large amplitude spikes with "pinching" in Fig. 1 *A*, may be lost when the cells are coupled. In modeling, neglecting coupling when matching experimental time courses could be misleading.

For both heterogeneous and stochastic clusters with uniform coupling, synchronized bursting occurs for coupling conductance > ~50–100 pS. As coupling increases above this threshold, burst period first increases to a maximum, and then declines. The initial increase in burst period is a consequence of the reduction of spike amplitude. The reason is as follows. Bursts are terminated when some slow negative-feedback variable (e.g., [ADP] in our model) increases to a critical level. When the threshold for spike activity rises to meet the plateau potential, the bursts end. Because spike amplitude is reduced at intermediate coupling, the plateau is raised, more inhibition is required, and the bursts increase in duration.

The reduction of spike amplitude and resulting increase in burst period has been previously described for pairs of identical bursters (25, Fig. 3). It was shown that for weak coupling in-phase spiking is unstable and the spikes lock 180° out-of-phase. For very strong coupling, the spikes synchronize in-phase, but for intermediate coupling no periodic, phase-locked behavior is stable; instead there are aperiodic oscillations of varying amplitude. The rapid amplitude modulation of the spikes in cell clusters (Fig. 2 *G*; reference 8, Fig. 2; and reference 29) appears to be related to this phenomenon. Recordings of spikes from two cells in islets (reference 27, Fig. 3) show some signs of this amplitude modulation and imperfect spike synchrony.

Coupling has been proposed (36) as a way to reconcile the slow bursts (5) and the slow Ca_i oscillations reported in isolated cells (36, 37) with the much faster bursts of membrane potential and Ca_i found in islets. These complex phenomena are beyond our scope here, but we see no basis in our study of electrical coupling effects for an increase in burst frequency; we find rather the opposite. We have not, however, considered the possibility that cells in islets experience a different chemical environment from isolated cells.

It has been suggested that cell variability has functional significance (4). The threshold distribution model for insulin secretion (14) assumes that the sigmoidal secretory response of islets to glucose is the result of a Gaussian-like distribution of thresholds for insulin packets or for cells. The latter variant has been emphasized recently (4). Our approach was to use the heterogeneous cluster model to derive the sigmoidal response from the electrical activity. We assumed a Gaussian distribution of the glucose-sensing parameter, R, rather than the secretory output. Lacking a secretory mechanism in the model, we measured the output, with and without coupling, in terms of the surrogate quantities mean plateau fraction and mean Ca_i levels. Fig. 5 shows that without coupling the glucose response is linear and shallow, whereas with coupling it is sigmoidal and sharp. The reduced response at low glucose (basal response) with coupling is due to suppression of the active cells by the silent cells. As glucose increases, enough cells become active to induce bursting, giving a clear threshold.

These results are consistent with experiments showing that the secretion dose–response curve of a coupled, large cluster or islet is considerably steeper than for isolated cells in suspension. Halban et al. (3; Fig. 1) found a 10-fold increase in secretion in islets when glucose was raised from 2.8 (subthreshold) to 16.7 mM (maximally stimulatory), whereas in isolated cells, the secretion at 2.8 mM was elevated fourfold relative to islets but was only increased another twofold at 16.7 mM. Allowing cells to reaggregate restored gap junctions, restored normal basal secretion, and partially restored the response to high glucose. It would be possible now to look for further experimental verification of this prediction of the model by measuring Ca_i levels in isolated cells and in

aggregates. Our model, of course, ignores the possibility of responses to glucose not dependent on membrane potential or Ca_i, and ignores any paracrine effects within the islet.

Note that in our model heterogeneity is *not* required for a glucose-sensing threshold; single cells that can burst also have a sharp dose–response curve (e.g., the mean cell, Fig. 5). What we have shown is that, in the presence of heterogeneity, nonlinear coupling interactions can produce a threshold where simple linear summation of heterogeneous responses does not.

We conclude that, far from merely acting to synchronize the electrical activity of pancreatic islets, gap junctional coupling profoundly shapes and modifies that electrical activity. This is seen in the emergence of bursting through mixing of cells with disparate properties, in the modification of spike patterns to increase burst period, and in the cooperation of differentially glucose-sensitive cells to produce a well-defined threshold for the glucose response. Thus, the dynamic repertoire of cells is enriched and rendered more robust and, perhaps, better suited to the biological role of regulating insulin secretion. We hope that this paper will motivate deeper experimental study of the comparative properties of isolated cells and islets.

We thank Dan Cook for encouraging us to think about reconciling heterogeneous cells with synchronized islets.

We acknowledge computer time provided by the National Cancer Institute Biomedical Supercomputing Center.

Received for publication 5 October 1992 and in final form 8 February 1993.

REFERENCES

1. Rorsman, P., and G. Trube. 1986. Calcium and delayed potassium currents in mouse pancreatic β-cells under voltage clamp conditions. *J. Physiol. (Lond.)*. 374:531–550.
2. Falke, L. C., K. D. Gillis, D. M. Pressel, and S. Misler. 1989. 'Perforated patch recording' allows long-term monitoring of metabolite-induced electrical activity and voltage-dependent Ca^{2+} currents in pancreatic islet B cells. *FEBS (Fed. Eur. Biochem. Soc.) Lett.* 251:167–172.
3. Halban, P., C. Wollheim, B. Blondel, P. Meda, E. Niesor, and D. Mintz. 1982. The possible importance of contact between pancreatic islet cells for the control of insulin release. *Endocrinology.* 111:86–94.
4. Pipeleers, D. 1987. The biosociology of pancreatic β-cells. *Diabetologia.* 30:277–291.
5. Smith, P. A., F. M. Ashcroft, and P. Rorsman. 1990. Simultaneous recordings of glucose dependent electrical activity and ATP-regulated K^+-currents in isolated mouse pancreatic β-cells. *FEBS (Fed. Eur. Biochem. Soc.) Lett.* 261:187–190.
6. Atwater, I., L. Rosario, and E. Rojas. 1983. Properties of calcium-activated potassium channels in the pancreatic β-cell. *Cell Calcium.* 4:451–461.
7. Sherman, A., J. Rinzel, and J. Keizer. 1988. Emergence of organized bursting in clusters of pancreatic β-cells by channel sharing. *Biophys. J.* 54:411–425.
8. Sherman, A., and J. Rinzel. 1991. Model for synchronization of pancreatic β-cells by gap junction coupling. *Biophys. J.* 59:547–559.
9. Chay, T. R., and H. S. Kang. 1988. Role of single-channel stochastic noise on bursting clusters of pancreatic β-cells. *Biophys. J.* 54:427–435.
10. Smolen, P., and J. Keizer. 1992. Slow voltage inactivation of Ca^{2+} currents and bursting mechanisms for the mouse pancreatic β-cell. *J. Membr. Biol.* 127:9–19.
11. Pipeleers, D., and M. Pipeleers-Marichal. 1981. A method for the purification of single A, B, or D cells and for the isolation of coupled cells from isolated rat islets. *Diabetologia.* 20:654–663.
12. Perez-Armendariz, M., C. Roy, D. C. Spray, and M. V. L. Bennett. 1991. Biophysical properties of gap junctions between freshly dispersed pairs of mouse pancreatic β-cells. *Biophys. J.* 59:76–92.
13. Rorsman, P., K. Bokvist, C. Ammala, P. Arkhammar, P. O. Berggren, O. Larsson, and K. Wahlander. 1991. Activation by adrenaline of a low-conductance G protein-dependent K^+ channel in mouse pancreatic β-cells. *Nature (Lond.)*. 349:77–79.
14. Grodsky, G. 1972. A threshold distribution hypothesis for packet storage of insulin and its mathematical modeling. *J. Clin. Invest.* 51:2047–2059.
15. Pipeleers, D., P. Veld, E. Maes, and M. Van De Winkel. 1982. Glucose-induced insulin release depends on functional cooperation between islet cells. *Proc. Natl. Acad. Sci. USA.* 79:7322–7325.
16. Pipeleers, D. 1992. Heterogeneity in pancreatic β-cell population. *Diabetes.* 41:777–781.
17. Chay, T. R., and J. Keizer. 1983. Minimal model for membrane oscillations in the pancreatic β-cell. *Biophys. J.* 42:181–190.
18. Hopkins, W., L. Satin, and D. L. Cook. 1991. Inactivation kinetics and pharmacology distinguish two calcium currents in mouse pancreatic β-cells. *J. Membr. Biol.* 119:229–239.
19. Satin, L., and D. L. Cook. 1989. Calcium current inactivation in insulin-secreting cells is mediated by calcium influx and membrane depolarization. *Pfluegers Arch. Eur. J. Physiol.* 414:1–10.
20. Valdeolmillos, M., R. Santos, D. Contreras, B. Soria, and L. Rosario. 1989. Glucose-induced oscillations of intracellular Ca^{2+} concentration resembling bursting electrical activity in single mouse islets of Langerhans. *FEBS (Fed. Eur. Biochem. Soc.) Lett.* 259:19–23.
21. Santos, R., L. Rosario, A. Nadal, J. Garcia-Sancho, B. Soria, and M. Valdeolmillos. 1991. Widespread synchronous Ca^{2+} oscillations due to bursting electrical activity in single pancreatic islets. *Pfluegers Arch. Eur. J. Physiol.* 418:417–422.
22. Keizer, J., and G. Magnus. 1989. ATP-sensitive potassium channels and bursting in the pancreatic β-cell. *Biophys. J.* 56:229–242.
23. Rojas, E., J. Hidalgo, P. Carroll, M.-X. Li, and I. Atwater. 1990. A new class of calcium channels activated by glucose in human pancreatic β-cells. *FEBS (Fed. Eur. Biochem. Soc.) Lett.* 261:265–270.
24. Eddlestone, G. T., A. Gonçalves, J. A. Bangham, and E. Rojas. 1984. Electrical coupling between cells in islets of Langerhans in mouse. *J. Membr. Biol.* 77:1–14.
25. Sherman, A., and J. Rinzel. 1992. Rhythmogenic effects of weak electrotonic coupling in neuronal models. *Proc. Natl. Acad. Sci. USA.* 89:2471–2474.
26. Meissner, H. P., and H. Schmelz. 1974. Membrane potential of

beta-cells in pancreatic islets. *Pfluegers Arch. Eur. J. Physiol.* 351:195–206.

27. Meissner, H. P. 1976. Electrophysiological evidence for coupling between beta cells of pancreatic islets. *Nature (Lond.)*. 262:502–504.
28. Rosario, L. M. 1983. Electrophysiological and ultra-violet irradiation studies on the pancreatic β-cells from normal and diabetic genetic background mice. Ph.D. thesis. School of Biological Sciences, University of East Anglia, Norwich, England.
29. Rinzel, J., A. Sherman, and C. L. Stokes. 1992. Channels, coupling, and synchronized rhythmic bursting activity. *In* Analysis and Modeling of Neural Systems. F. Eeckman, editor. Kluwer Academic Publishers, Boston. 29–46.
30. Eddlestone, G. T. 1980. An electrophysiological study on the β-cell of the islet of Langerhans from the mouse. Ph.D. thesis. School of Biological Sciences, University of East Anglia, Norwich, England.
31. Dean, P. M., and E. K. Matthews. 1968. Electrical activity in pancreatic islet cells. *Nature (Lond.)*. 219:389–390.
32. Van De Winkel, M., and D. Pipeleers. 1983. Autofluorescence-activated cell sorting of pancreatic islet cells: purification of insulin-containing B-cells according to glucose-induced changes in cellular redox state. *Biochem. Biophys. Res. Commun.* 114:835–842.
33. Fitzhugh, R. 1961. Impulses and physiological states in theoretical models of nerve membrane. *Biophys. J.* 1:445–466.
34. Halloy, J., Y. X. Li, J. L. Martiel, B. Wurster, and A. Goldbeter. 1990. Coupling chaotic and periodic cells results in a period-doubling route to chaos in a model for cAMP oscillations in *Dictyostelium* suspensions. *Phys. Lett. A.* 151:33–36.
35. Kukuljan, M., A. Goncalves, and I. Atwater. 1991. Charybdotoxin-sensitive K-Ca channel is not involved in glucose-induced electrical activity of pancreatic β-cells. *J. Membr. Biol.* 119:187–195.
36. Gylfe, E., E. Grapengiesser, and B. Hellman. 1991. Propagation of cytoplasmic Ca^{2+} oscillations in clusters of pancreatic β-cells exposed to glucose. *Cell Calcium.* 12:229–240.
37. Grapengiesser, E., E. Gylfe, and B. Hellman. 1989. Three types of cytoplasmic Ca^{2+} oscillations in stimulated pancreatic β-cells. *Arch. Biochem. Biophys.* 268:404–407.